Figures and tables

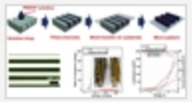

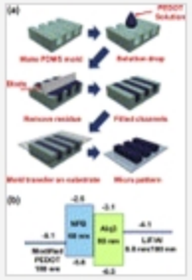

Table 1

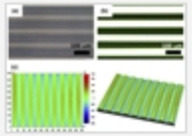

Organic Electronics
Volume 14, Issue 1, January 2013, Pages 416–422

Letter

Negative mold transfer patterned conductive polymer electrode for flexible organic light-emitting diodes

Hyun Jun Lee[a], Tae Hyun Park[a], Jin Hwan Choi[a], Eun Ho Song[a], Se Joong Shin[a], Hakkoo Kim[a], Kyung Cheol Choi[b], Young Wook Park[c, 1], Byeong-Kwon Ju[a]

Show more

http://dx.doi.org/10.1016/j.orgel.2012.11.015

Abstract

We demonstrate flexible organic light-emitting diodes (FOLEDs) that use flexible conductive polymer electrodes patterned by negative mold transfer printing (nMTP). Because pristine poly(3,4-ethylenedioxythiophene):poly(styrenesulfonate) (PEDOT:PSS) is unsuitable for nMTP owing to problems with wettability, additives are used to improve the surface wetting properties of the polymer on the mold to successfully employ nMTP. Moreover, the additives improve the conductivity of the polymer electrode. FOLEDs fabricated with the modified PEDOT:PSS using nMTP exhibit electrical properties comparable to those of a device having an indium tin oxide (ITO) anode. These results show that the highly conductive PEDOT:PSS patterned by nMTP can be used as transparent high-resolution electrodes in low-cost ITO-free FOLEDs.

Graphical abstract

Organic Electronics 14 (2013) 416–422

Contents lists available at SciVerse ScienceDirect

Organic Electronics

journal homepage: www.elsevier.com/locate/orgel

Letter

Negative mold transfer patterned conductive polymer electrode for flexible organic light-emitting diodes

Hyun Jun Lee [a], Tae Hyun Park [a], Jin Hwan Choi [a], Eun Ho Song [a], Se Joong Shin [a], Hakkoo Kim [a], Kyung Cheol Choi [b], Young Wook Park [c,1], Byeong-Kwon Ju [a,*]

[a] Display and Nanosystem Laboratory, College of Engineering, Korea University, Seoul 136-713, Republic of Korea
[b] Department of Electrical Engineering, KAIST, Daejeon 305-701, Republic of Korea
[c] The Institute of High Technology Materials and Devices, Korea University, Seoul 136-713, Republic of Korea

ARTICLE INFO

Article history:
Received 28 August 2012
Received in revised form 15 November 2012
Accepted 18 November 2012
Available online 6 December 2012

Keywords:
Negative mold transfer printing (nMTP)
Conductive polymer
Micropatterning
Transparent
Flexible organic light-emitting diode (FOLED)

ABSTRACT

We demonstrate flexible organic light-emitting diodes (FOLEDs) that use flexible conductive polymer electrodes patterned by negative mold transfer printing (nMTP). Because pristine poly(3,4-ethylenedioxythiophene):poly(styrenesulfonate) (PEDOT:PSS) is unsuitable for nMTP owing to problems with wettability, additives are used to improve the surface wetting properties of the polymer on the mold to successfully employ nMTP. Moreover, the additives improve the conductivity of the polymer electrode. FOLEDs fabricated with the modified PEDOT:PSS using nMTP exhibit electrical properties comparable to those of a device having an indium tin oxide (ITO) anode. These results show that the highly conductive PEDOT:PSS patterned by nMTP can be used as transparent high-resolution electrodes in low-cost ITO-free FOLEDs.

1. Introduction

Flexible organic light-emitting diodes (FOLEDs) have attracted much attention because of their potential for mass production, large-area applications, and low-cost processing [1]. Although indium tin oxide (ITO) has generally been used as the transparent electrode in OLEDs, its rarity, high cost, and lack of flexibility make it unsuitable for flexible devices [2]. Therefore, to achieve high device performance and reduce the production cost, it is necessary to consider alternative electrode materials.

Among the various conducting polymers, poly(3,4-ethylenedioxythiophene):poly(styrenesulfonate) (PEDOT:PSS) has attracted considerable attention because of its relatively low cost, transparency, and high flexibility [3]. To realize high-performance ITO-free devices, which is not possible with pristine PEDOT:PSS, a number of groups are currently attempting to improve the conductivity of PEDOT:PSS. For this reason, over the past few years, many researchers have investigated how its electrical properties can be enhanced with polyalcohol or polar solvents such as dimethyl sulfoxide (DMSO) [4], ethylene glycol [5], and glycerol [6]. At the same time, the realization of high-resolution patterned conductive polymer electrodes has also been a key issue for optical electronics, including future OLEDs. Many research studies have examined the high-resolution patterning of polymer electrodes via inkjet printing [7], mold transfer printing (MTP) [8], screen printing [9], and micro-contact printing (μCP) [10]. However, these methods have several problems. In inkjet printing, the nozzles on the head are easily clogged. Additionally, some printing techniques require the removal of the residual layer for post-imprinting steps.

The negative mold transfer printing (nMTP) method has many advantages over other techniques in the industrial

* Corresponding author.
E-mail addresses: zerook@korea.ac.kr (Y.W. Park), bkju@korea.ac.kr (B.-K. Ju).
[1] Co-corresponding author.

1566-1199/$ - see front matter © 2012 Elsevier B.V. All rights reserved.
http://dx.doi.org/10.1016/j.orgel.2012.11.015

production of polymer electrodes. It is possible to print fine patterns without high vacuum conditions or a photolithography process; additionally, it is a simple solution processing technique that is scalable to very large samples. Moreover, it can be used to generate isolated micro/nano-structures in various electronic devices instead of the previously reported continuous micro/nano-structures [11]. Hwang et al. demonstrated the fabrication of a few nano-scale and hundreds of micro-scale structures and thin-film transistors by a mold transfer process [12]. Because of its differences from many other common imprinting techniques, nMTP is a valuable and promising technique for micro-nano devices. Despite the aforementioned advantages, it is usually difficult to find suitable polymers, or mixed polymers including the foregoing conductivity-enhancing additives, for use in the nMTP process. First, and most importantly, the wetting behavior of solutions is an important factor in the imprinting process [13]. For example, Eom et al. reported that PEDOT:PSS with additives improved both the surface morphology and the conductivity, resulting in enhanced photovoltaic performance using an inkjet-printing process [14]. As mentioned above, the pristine PEDOT:PSS cannot be coated on an intaglio part of polydimethylsiloxane (PDMS) for nMTP, because dewetting on the hydrophobic surface of PDMS leads to droplet formation. For this reason, the wettability of the polymers must be adjusted to match the filling channels used for nMTP. If the wetting properties of the solution are not controlled, uneven patterns occur partially because of inappropriate arrangement of the polymer in the intaglio part. For this reason, successful application of conductive polymers to nMTP for the production of FOLEDs is almost never reported. To solve this problem, we tried to modify PEDOT:PSS by adding a solvent to achieve both appropriate wettability for nMTP and the electrical properties required of electrodes in electronic devices. After numerous attempts, we found a suitable PEDOT:PSS solution that could be modified not only for use with nMTP but also for enhancing the electrical properties. In addition, all substrates were treated with oxygen plasma for successful transfer.

The modified PEDOT:PSS electrode showed a sheet resistance of less than 55 Ω/sq and greater than 80% transmittance in the visible spectrum while maintaining high flexibility; subsequently, high-resolution patterned FOLEDs were successfully fabricated using nMTP.

In this work, we used a modified PEDOT:PSS solution to improve the conductivity; we present the first demonstration of the nMTP technique not only for the anode in FOLEDs, but also for alignment control of a multilayered PEDOT:PSS electrode produced entirely by nonvacuum processes. Furthermore, the nMTP technique, which is capable of nano-scale high-resolution patterning, will pave the way for production of the highly anticipated augmented reality head-mounted display [15].

2. Experimental

To fabricate the mold and stamps, PDMS (Sylgard 184, Dow Corning) was prepared by mixing the base and curing agent in the weight ratio 10:1. The PDMS mixture was poured onto a micropatterned silicon wafer substrate and cured for 3 h at 70 °C. The modified PEDOT:PSS solution for the electrode had a composition of PEDOT:PSS (Clevios PH1000, H.C. Starck) mixed with glycerol (Sigma–Aldrich) and surfynol (Air Products) in the ratio 5 wt%:1 wt%. Glycerol and surfynol were used as a conduction-enhancing additive and a surfactant, respectively. The solution was stirred for 1 h, sonicated for 20 min, and then filtered with polyvinylidene difluoride 0.45 μm syringe filters (Whatman).

To evaluate the physical, electrical, optical, and flexibility characteristics of the modified PEDOT:PSS solution, a thin film of PEDOT:PSS was spin-coated on glass and polyethersulfone substrates at 1500 rpm for 40 s and subsequently annealed on a hot plate at 120 °C for 20 min. Glass substrates were precleaned by ultrasonication in acetone, methanol, and deionized water; cleaned for 5 min each; and treated with oxygen plasma under 50 sccm of oxygen and 100 W for 50 s (Cute-MP, Femto Science). In addition, polyethersulfone substrates were precleaned by the same process without acetone treatment.

The contact angles of deionized water and formamide relative to various films were measured using a contact angle goniometer (Phoenix-450, SEO) for accurate measurement. The contact angles were measured after 5 s, and the averaged value was taken from 10 different points on the samples. The sheet resistances of the films were measured using a four-point probe with a source measurement unit (Keithley 2400). The sheet resistance of each sample was measured 10 times and then averaged. The transmittance characteristics were measured using a UV–vis spectrophotometer (Cary 5000, Varian) in the wavelength range of 300–800 nm. The surface morphologies of the PEDOT:PSS films were measured by atomic force microscopy (AFM, XE-100, Park Systems) in noncontact mode. A cyclic bending test of the PEDOT:PSS anodes and ITO anodes was conducted in a bending machine (ZB100, Z-Tech) to clarify the flexibility characteristics of the modified PEDOT:PSS films. The samples were measured immediately after preparation.

Fig. 1a illustrates this process for creating the micropatterned electrode. A modified PEDOT:PSS electrode as an anode electrode was patterned by nMTP. The prepared modified PEDOT:PSS solution was dropped onto an intaglio-patterned PDMS mold, and the residual solution on the embossed surface of the PDMS was removed using a blade. The PDMS mold filled with the modified solution was preannealed on a hot plate at 80 °C for 3 min and then transferred to the top of the substrate in order to transfer the PEDOT:PSS solution. Controlled pressure was applied by using μCP equipment at 120 °C for 20 min to ensure that the contact region at the interface was as conformable as possible. When the PDMS mold was released, the solution of the intaglio part was transferred onto the substrate, forming the line electrode micropattern. In addition, the microstructure was measured for definition of the pattern by an optical profiling system with VSI mode (Wyko NT1100, Veeco).

Two types of OLEDs were fabricated to evaluate the characteristics of the conductive polymer as an anode

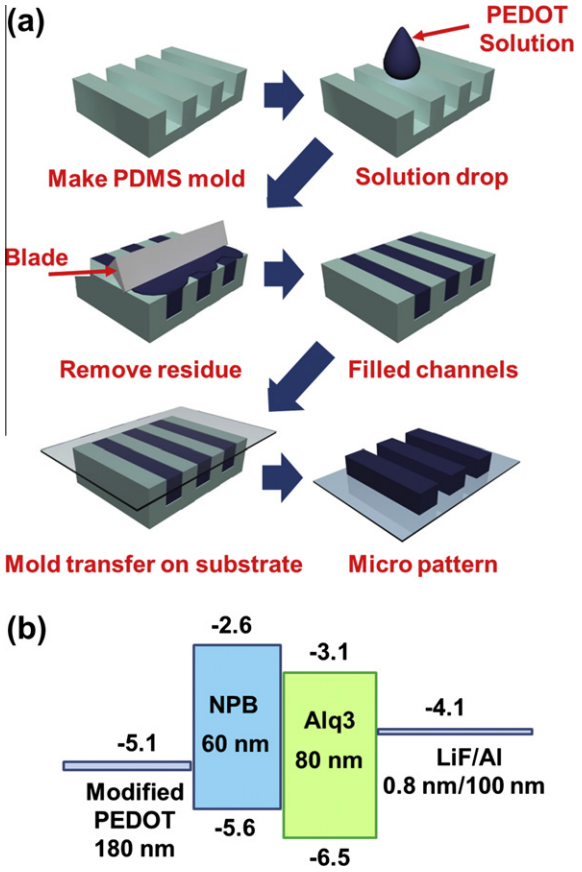

Fig. 1. Mold-transferred PEDOT:PSS conductive polymer electrode: (a) fabrication process using mold transfer printing, (b) energy level diagram and device structure of the fabricated OLEDs.

electrode in OLEDs. As a reference device, OLEDs were fabricated using a commercial ITO-coated substrate. A reference device on top of the ITO anodes was fabricated by thermal evaporation in a high vacuum ($\sim 2 \times 10^{-6}$ torr). The modified PEDOT:PSS anode produced by the nMTP technique was under normal atmospheric conditions. The structure of the OLED device employed in this study is shown in Fig. 1b. An organic structure consisting of N,N-bis(naphthalene-1-yl)-N,N-bis(phenyl)-benzidine (NPB) (60 nm) was used as a hole transport layer, and (8-hydroxy-quinolinato)-aluminum (Alq3) (80 nm) was used as both an emission layer and an electron transport layer. Finally, 0.8 nm of lithium fluoride (LiF) and 100 nm of aluminum were deposited on the organic layers as an electron injection layer and as a cathode, respectively. The deposition rates of all of the organic materials and metals were ~1 Å/s and ~6 Å/s, respectively. The active emission area of the devices was 5 mm × 5 mm. The EL characteristics of the fabricated OLEDs were measured by using a high-voltage source measurement unit (Model 237, Keithley Instruments) and a spectroradiometer (PR-670SpectraScan, Photo Research) at room temperature without any passivation layer in a dark box.

3. Results and discussion

To evaluate the wetting properties of the polymer-coated thin film, the contact angle was measured with a polar liquid (deionized water); it was 47° on the pristine PEDOT:PSS and decreased to 10° on the modified PEDOT:PSS. As summarized in Table 1, the addition of glycerol to the PEDOT:PSS solution increased the static surface energy to 55.04 mJ/m^2. As expected from the measured contact angles, the addition of surfynol produced a further increase from 55.04 mJ/m^2 to 72.3 mJ/m^2. One might expect surfynol (a surfactant) to become more effective with increasing contact area. The decrease in the water contact angle indicates that the surface of the modified PEDOT:PSS became broadly more hydrophilic.

Consequently, the modified PEDOT:PSS was finely patterned using nMTP. Fig. 2a shows an optical image of the finely patterned lines of the modified PEDOT:PSS electrode. As shown in Fig. 2b, OLEDs having finely patterned PEDOT:PSS electrodes produce a clear line emission image at 8 V. As shown in Fig. 2c, the measurement of the optical profiler shows a patterned line of the modified PEDOT:PSS that can be achieved by nMTP. Additionally, the three-dimensional interactive image shows uniform resolution (the line width is 45 μm, height is 200 nm, and length 25 mm). In addition, this process demonstrated easy control of the alignment of the PEDOT:PSS electrode with another layer in an entirely nonvacuum process, as shown in Fig. 3.

As mentioned above, the addition of surfynol improves not only the wetting properties of PEDOT:PSS solutions on a mold by matching the surface energy but also increases the conductivity of PEDOT:PSS films from ~0.37 S/cm to ~4.69 S/cm. Nevertheless, the conductivity of the film modified only by surfynol was not sufficient for application as an efficient OLED anode. To solve this problem, glycerol was added as a supplement to produce an increased conductivity of 1010 S/cm [16].

To determine the mechanism of the conductivity enhancement of the PEDOT:PSS films, we employed AFM in noncontact mode to characterize the origin of the conductivity enhancement by measuring the topographies

Table 1
Conductivity and surface wetting properties of PEDOT:PSS films with various additives.

	Pristine	Added 4% glycerol	Added 1% surfynol	Modified
Conductivity (S/cm)	0.37	92.93	4.69	1010
Contact angle (water/formamide) (°)	47/34	43/32	13/10	10/9
Dispersion energy (mJ/m^2)	21.93	20.52	17.12	16.78
Polar energy (mJ/m^2)	30.5	34.51	54.32	55.51
Surface energy (mJ/m^2)	52.44	55.04	71.45	72.30

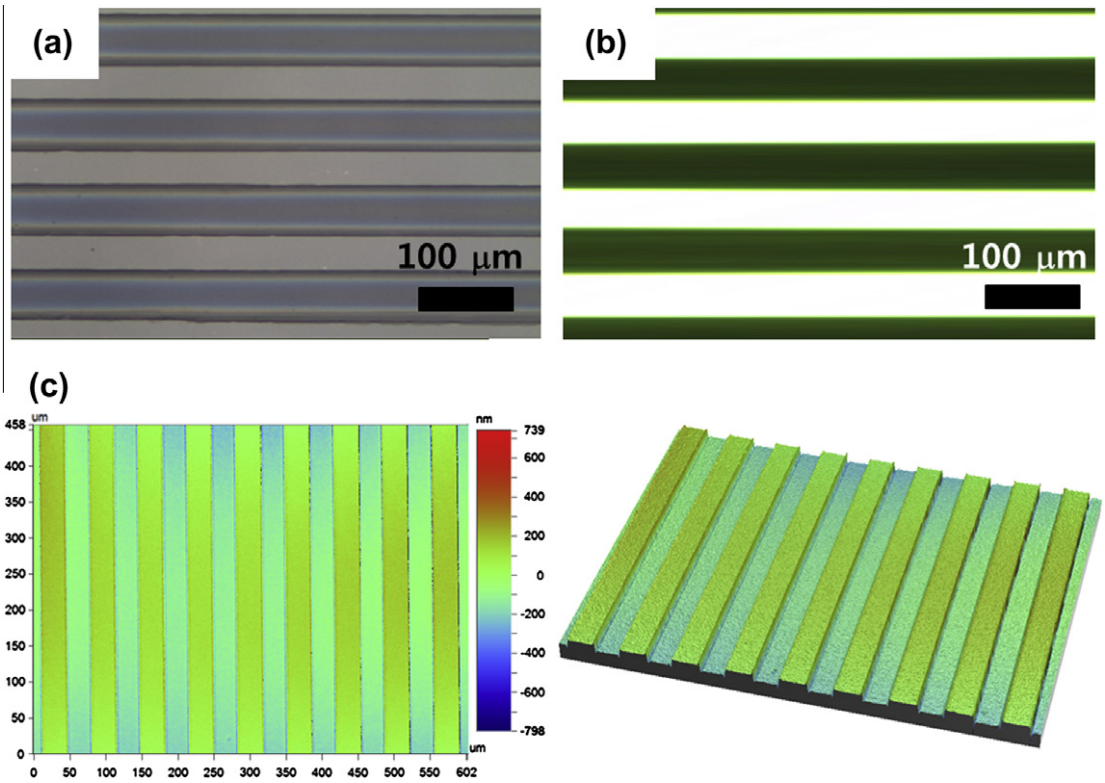

Fig. 2. Micropatterned conductive electrode: (a) optical image of line-patterned PEDOT:PSS electrode, (b) photo of emission from fabricated OLEDs at 8 V, (c) optical profiler image of the transferred microstructure and three-dimensional interactive image.

Fig. 3. Alignment control images of PEDOT:PSS electrode on another layer.

and phase diagrams of a pristine PEDOT:PSS (PH1000) film and the PEDOT:PSS film with 4 wt% glycerol and 1 wt% surfynol coated on glass substrates (1 μm × 1 μm). AFM topography images of the pristine and modified PEDOT:PSS films are shown in Fig. 4a and c, respectively. It is evident that the glycerol and surfynol changed the surface root-mean-square roughness (R_q) from 1.05 to 2.18 nm. The foregoing AFM analysis indicated an increase in the PEDOT grain size.

Changes in the grain size and structure of polymers generally affect the conductivity [17]. It is clear from Fig. 4b and d that the decrease in the sheet resistance of the PEDOT:PSS films is because the larger PEDOT grains provide larger regions, which is supported by the fact that the modified PEDOT films have a better interconnected PEDOT grain structure than the corresponding pristine PEDOT films [18]. For this reason, the formation of linear PEDOT chains produced a film with more continuous and stronger inter-chain networks [19]. These structural changes modified the conductivity of the pristine PEDOT:PSS film. Consequently, the controlled additives generated better-oriented PEDOT-rich grains, which improved the electrical characteristic for carriers by enhancing the conducting pathway [20]. In addition, Alemu et al. reported the effects of additives on PEDOT organization and improvement in the PEDOT film's

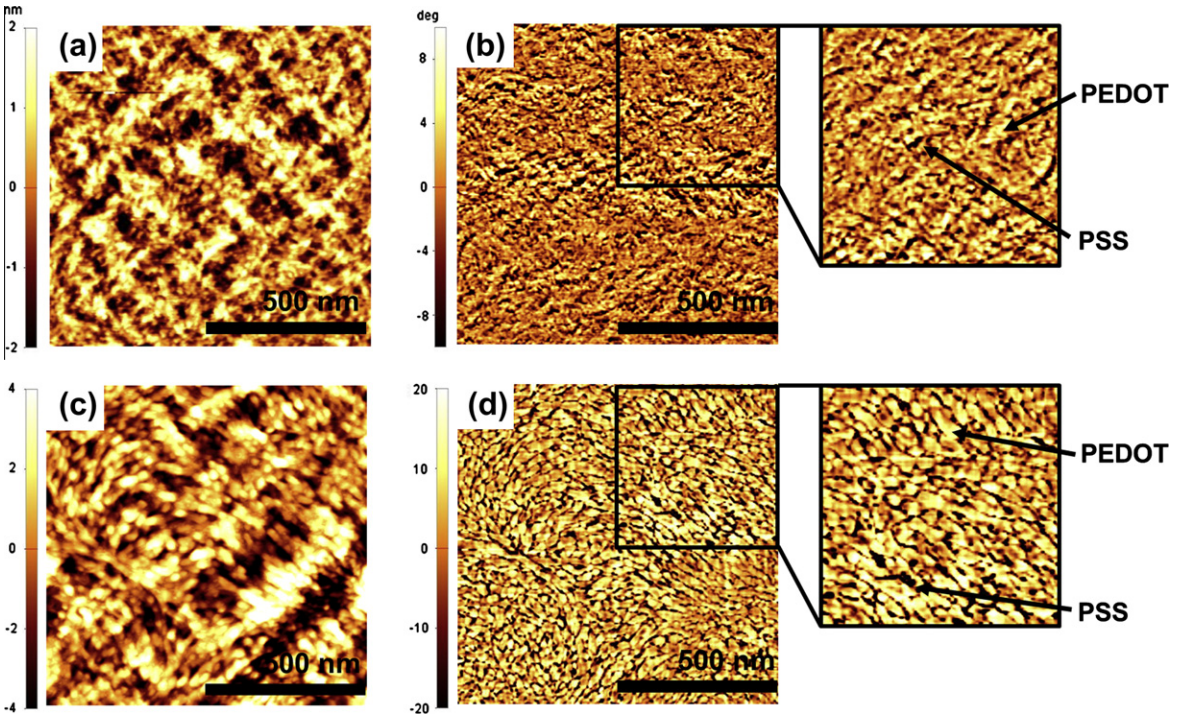

Fig. 4. AFM topographic (a, c) and phase (b, d) images of pristine PEDOT-PSS and modified PEDOT:PSS films (1 μm × 1 μm).

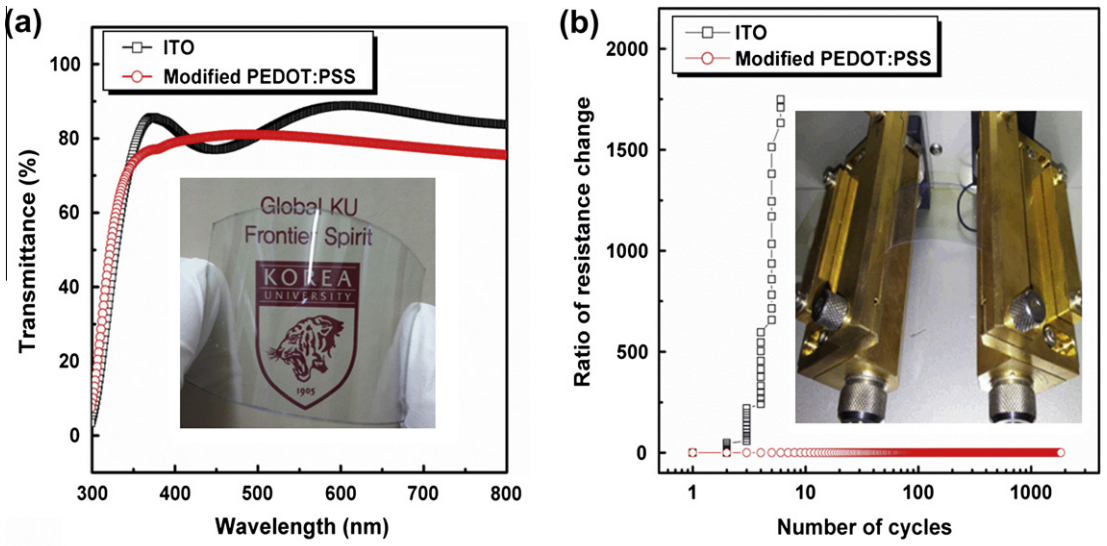

Fig. 5. Characteristics of PEDOT:PSS films: (a) optical transmittance and photograph of this flexible film, (b) ratio of resistance changes in the bending test and photograph of the bending tester measuring the flexibility of the film.

long-term stability [21]. In other words, additives changed the PEDOT grain size and composition, which affect not only the conductivity but also the stability of the film. The modified stability of the film has a significant influence on the long-term performance of an OLED device.

Fig. 5a shows the transmittance of the modified PEDOT:PSS films and ITO (as a reference). The modified film shows ~80% transmittance in the visible wavelength region (film thickness 180 nm). Fig. 5b shows the flexibility characteristics of the modified PEDOT:PSS flexible conductive films and ITO. The test was performed with a bending length of 20 mm and bending radius of 3 mm. The ratio of the change in the resistance of the electrodes was recorded as a function of the bending cycle; the resistance changes were recorded 10 times at each bending cycle for accurate

Table 2
Electrical characteristics of films and OLEDs with anodes of ITO (I-OLED) and modified PEDOT:PSS (P-OLED).

Configuration	Sheet resistance (Ω/sq)	Work function (eV)	At 1000 cd/m^2		At 10 mA/cm^2	
			EQE (%)	PE (lm/W)	EQE (%)	PE (lm/W)
I-OLED	10	4.6 (Ref. [20])	1.18	1.38	1.12	1.37
P-OLED	55	5.1 (Ref. [19])	1.37	1.6	1.37	1.79

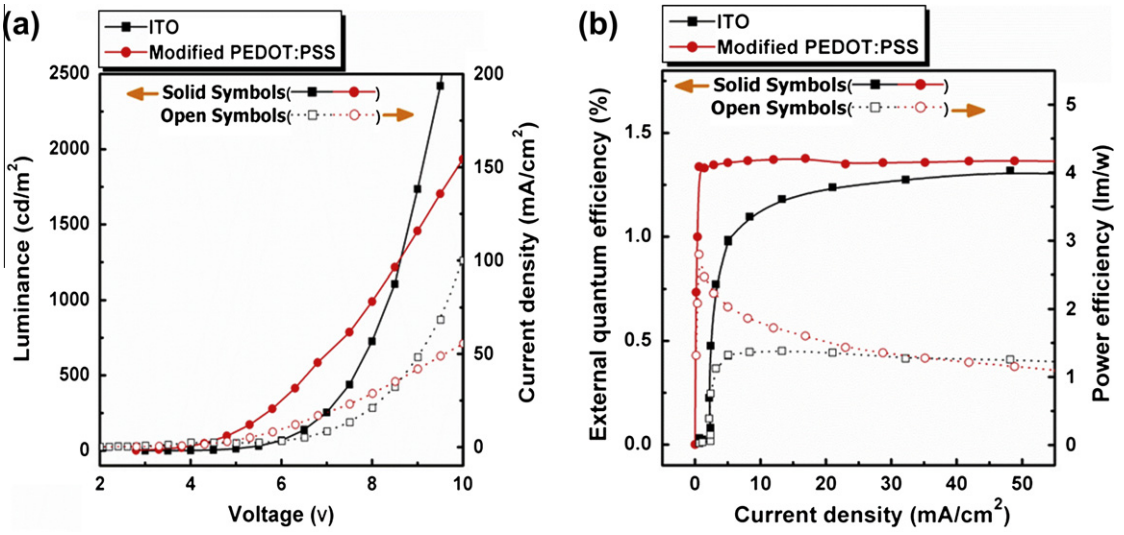

Fig. 6. Electrical properties of devices: (a) luminance and current density characteristics as a function of bias voltage, (b) external quantum efficiency and power efficiency as a function of applied current density.

measurement. ITO films are well known to be fragile and inflexible [22]; consequently, the ratio of the resistance changes of the ITO film could not be measured after six bending cycles. In contrast, the modified PEDOT:PSS film exhibited stable electrical performance through more than 1000 bending test cycles.

Fig. 5 and Table 2 show the electroluminescence characteristics of OLEDs with a modified PEDOT:PSS anode (P-OLEDs) and reference OLEDs with an ITO anode (I-OLEDs). The P-OLED exhibited a lower turn-on voltage (2.8 V) than the I-OLED (Fig. 6a). This difference is attributed to a difference in the work function. The high work function of the PEDOT:PSS anode electrode (5.1 eV) [23], which is advantageous for hole injection compared to the work function of ITO (4.6 eV) [24], decreases the turn-on voltage of the device. The P-OLEDs exhibited higher brightness than the I-OLEDs at low voltage; in contrast, the luminance of the I-OLEDs was higher than that of the P-OLEDs at more than 9 V because PEDOT:PSS has a higher sheet resistance than ITO. For these reasons, as shown in Fig. 6b, the P-OLEDs exhibited a higher external quantum efficiency and power efficiency than the I-OLEDs at low current density. The results show that the OLEDs developed here can be used for low-cost organic electronics in low-voltage driving applications.

The results show that the modified PEDOT:PSS films exhibited enhanced electrical properties and were capable of patterning; consequently, they show promise as flexible transparent electrodes [25].

4. Conclusion

In conclusion, we successfully demonstrated the patterning of PEDOT:PSS electrodes by nMTP for use as anodes in FOLEDs.

The pristine PEDOT:PSS films had unsuitable wetting properties for nMTP. To solve this problem, additives were used to enhance their wettability and electrical properties. The wetting characteristics of the modified solvents on the mold were singularly suitable for the use of nMTP for fine patterning.

To produce a promising conductive polymer electrode, various key factors such as the transparency, conductivity, work function, and solution process ability should have satisfactory values. When these factors have suitable values, the demonstrated highly efficient P-OLEDs can be produced by a simple device process with lower manufacturing costs.

Most importantly, nMTP using the modified PEDOT:PSS is an economical process compared to that using ITO because it requires no high-vacuum or photolithography process and can be adopted for large-area transfer. In addition, as reported, high-resolution nanopatterning and isolated

micro/nano-structures for various electronic devices can be generated. Therefore, nMTP can be adopted for the mass production of high-resolution FOLEDs without a vacuum process.

These results clearly demonstrate that the use of nMTP for transparent conductive polymers can be expected to enable the development of a broadly applicable printing technology in the OLED industry and to play an important role in the dissemination of low-cost, high-performance devices. Our results indicate the possibility of nMTP emerging as a promising technique for large-scale area and flexible devices.

Acknowledgements

This research was supported by the Basic Science Research Program through the National Research Foundation of Korea (NRF) funded by the Ministry of Education, Science and Technology (MEST) (CAFDC-20120000816), the NRF (No. 2012R1A6A3A04039396) Project of the MEST, and the IT R&D Program of MKE/KEIT (No. 2009-F-016-01, Development of Eco-Emotional OLED Flat-Panel Lighting). The authors thank the staff of KBSI for technical assistance.

References

[1] S. Logothetidis, Mater. Sci. Eng. B. 152 (2008) 96–104.
[2] D.R. Cairns, R.P. Witte, D.K. Sparacin, S.M. Sachsman, D.C. Paine, G.P. Crawford, R.R. Newton, Appl. Phys. Lett. 76 (2000) 1425–1427.
[3] M.S. Lee, H.S. Kang, H.S. Kang, J. Joo, A.J. Epstein, J.Y. Lee, Thin Solid Films 477 (2005) 169–173.
[4] Y. Yim, J. Park, B. Park, J. Disp. Technol. 6 (2010) 252–256.
[5] M.W. Lee, M.Y. Lee, J.C. Choi, J.S. Park, C.K. Song, Org. Electron. 11 (2010) 854–859.
[6] K.H. Tsai, S.C. Shiu, C.F. Lin, Proc. SPIE 7052 (2008) 70521 B.
[7] Y. Yoshioka, P.D. Calvert, G.E. Jabbour, Macromol. Rapid Commun. 26 (2005) 238–246.
[8] N. Unno, J. Taniguchi, Microelectron. Eng. 87 (2010) 1019–1023.
[9] D. Nilsson, T. Kugler, P.-O. Svensson, M. Berggren, Sens. Actuators B: Chem. 86 (2002) 193–197.
[10] T.-Y. Oh, N.-S. Kang, K.-Y. Dong, S. Chang, J.-H. Park, S.-W. Jung, S.-J. Lee, B.-K. Ju, Phys. Status Solidi RRL 5 (2011) 101–103.
[11] J.P. Rolland, E.C. Hagberg, G.M. Denison, K.R. Carter, J.M. DeSimone, Chem. Int. Ed. 43 (2004) 5796–5799.
[12] J.K. Hwang, S. Cho, J.M. Dang, E.B. Kwak, K. Song, J. Moon, M.M. Sung, Nat. Nanotechnol. 5 (2010) 742–748.
[13] D. Zhang, D.H. Gracias, R. Ward, M. Gauckler, Y. Tian, Y.R. Shen, G.A. Somorjai, J. Phys. Chem B. 102 (1998) 6225–6230.
[14] S.H. Eom, S. Senthilarasua, P. Uthirakumar, S.C. Yoon, J. Lim, C. Lee, H.S. Lim, J. Lee, S.H. Lee, Org. Electron. 10 (2009) 536–542.
[15] O. Cakmakci, J. Rolland, J. Display Technol. 2 (2006) 199–216.
[16] S.L. Lai, M.Y. Chan, M.K. Fung, C.S. Lee, S.T. Lee, Mater. Sci. Eng. B. 104 (2003) 26–30.
[17] J. Huang, P.F. Miller, J.C. de Mello, A.J. de Mello, D.D.C. Bradley, Synthetic Met. 139 (2003) 569–572.
[18] U. Lang, E. Müller, N. Naujoks, J. Dual, Adv. Funct. Mater. 19 (2009) 1215–1220.
[19] Y. Hsiao, W. Whang, C. Chen, Y. Chen, J. Mater. Chem. 18 (2008) 5948–5955.
[20] Y.H. Kim, C. Sachse, M.L. Machala, C. May, L. Müller-Meskamp, K. Leo, Adv. Funct. Mater. 21 (2011) 1076–1081.
[21] D. Alemu, H.-Y. Wei, K.-C. Ho, C.-W. Chu, Energy Environ. Sci. 5 (2012) 9662–9671.
[22] J.W. Huh, Y.M. Kim, Y.W. Park, J.H. Choi, J.W. Lee, J.W. Lee, J.W. Yang, S.H. Ju, K.K. Paek, B.K. Ju, J. Appl. Phys. 103 (2008) 044502.
[23] X. Crispin, F.L.E. Jakobsson, A. Crispin, P.C.M. Grim, P. Andersson, A. Volodin, C. Van Haesendonck, M. Van der Auweraer, W.R. Salaneck, M. Berggren, Chem. Mater. 18 (2006) 4354–4360.
[24] H. Mu, W. Li, R. Jones, A. Steckl, D. Klotzkin, J. Luminescence 126 (2007) 225–229.
[25] M.C. Choi, Y. Kim, C.S. Ha, Prog. Polym. Sci. 33 (2008) 581–630.